

Original Article
Urology



Pattern Analysis of Laser Fiber Degradation According to the Laser Setting: In Vitro Study of the Double-Firing Phenomenon

Gyoohwan Jung ,¹ Seung Min Lee ,² Sang Won So ,² Sehwan Kim ,² Seong Chan Kim ,³ Ohbin Kwon ,³ Hyunjae Song ,⁴ Min Joo Choi ,^{3,5} and Sung Yong Cho ^{2,6}

¹Department of Urology, Seoul National University Bundang Hospital, Seongnam, Korea

²College of Medicine, Seoul National University, Seoul, Korea

³Interdisciplinary Postgraduate Program in Biomedical Engineering, Jeju National University, Jeju, Korea

⁴Department of Electronic Engineering, Sogang University, Seoul, Korea

⁵Department of Medicine, School of Medicine, Jeju National University, Jeju, Korea

⁶Department of Urology, Seoul National University Hospital, Seoul, Korea



Received: Apr 6, 2022

Accepted: Aug 3, 2022

Published online: Sep 16, 2022

Address for Correspondence:

Sung Yong Cho, MD, PhD

Department of Urology, Seoul National University Hospital, 101 Daehak-ro, Jongno-gu, Seoul 03080, Korea.

Email: kmoretry@daum.net

© 2022 The Korean Academy of Medical Sciences.

This is an Open Access article distributed under the terms of the Creative Commons Attribution Non-Commercial License (<https://creativecommons.org/licenses/by-nc/4.0/>) which permits unrestricted non-commercial use, distribution, and reproduction in any medium, provided the original work is properly cited.

ORCID iDs

Gyoohwan Jung

<https://orcid.org/0000-0002-1602-0036>

Seung Min Lee

<https://orcid.org/0000-0002-3419-3336>

Sang Won So

<https://orcid.org/0000-0002-9428-4272>

Sehwan Kim

<https://orcid.org/0000-0001-6058-9687>

Seong Chan Kim

<https://orcid.org/0000-0001-9377-3632>

Ohbin Kwon

<https://orcid.org/0000-0002-4422-9478>

ABSTRACT

Background: It is essential to understand the mechanism of the various causes of laser fiber damage and an ideal method of reducing endoscope damage induced by laser emission in multiple sites. This study classified the different patterns of laser fiber degradation according to laser settings and analyzed the role of cavitation bubbles to find a desirable way of minimizing endoscope damage.

Methods: A total of 118 laser fibers were analyzed after 1-, 3-, and 5-min laser emission to artificial stones under the settings of 1 J-10 Hz, 1 J-20 Hz, 1 J-30 Hz, and 2 J-10 Hz. Every 3 cm from the fiber tip was marked and examined with a digital microscope and a high-speed camera. The images of the fibers and the movement of cavitation bubbles were taken with a distance of 1 to 5 mm from the gel.


Results: Seven types of fiber damage (charring, limited and extensive peeled-off, bumpy, whitish plaque, crack, and break-off) coincided during laser emission. Damages rapidly increased with emission time > 3 minutes regardless of the laser settings. The damaged lengths covered 5 mm on average, and the fibers at 5-min emission were significantly shorter than others. The fiber durability of 1J-10Hz setting was better than other settings after 3-min laser emission. Backward movement of the cavitation bubbles was found at the 1-mm distance from the gel, and the damaged lengths were longer than the diameters of the cavitation bubbles because of their proximal movement.

Conclusion: The damage patterns of the laser fiber tips were classified into seven types. The heat damage around the surface of the laser fiber can be increased according to the high-energy or high-frequency laser setting, a short distance to the stone, a short distance from the tips of flexible ureteroscopes, no cutting laser fiber procedures, and the inappropriate use of irrigation fluid or laser fiber jacket.


Keywords: Ureteroscopes; Lasers; Pattern of Degradation

Hyunjae Song 

<https://orcid.org/0000-0001-7469-0700>

Min Joo Choi 

<https://orcid.org/0000-0003-4626-3706>

Sung Yong Cho 

<https://orcid.org/0000-0001-9271-6951>

Funding

This work was supported by the Korea Medical Device Development Fund grant funded by the Korean government (the Ministry of Science and ICT, the Ministry of Trade, Industry and Energy, the Ministry of Health & Welfare, the Ministry of Food and Drug Safety) (Project Number: KMDF_PR_20200901_0010, 1711134986) (KMDF-RnD, NTIS 202011B04) and, in part, National Research Foundation of Korea (2019R1C1C1008339).

Disclosure

The authors have no potential conflicts of interest to disclose.

Author Contributions

Conceptualization: Jung G, Cho SY. Data curation: Jung G. Formal analysis: Lee SM, So SW, Kim S. Funding acquisition: Cho SY. Investigation: Kwon O, Song H. Methodology: Choi MJ, Cho SY. Software: Cho SY. Validation: Kim SC, Kwon O, Song H, Choi MJ. Visualization: Jung G. Writing - original draft: Jung G. Writing - review & editing: Lee SM, So SW, Kim S, Choi MJ, Cho SY.

INTRODUCTION

Flexible ureteroscopy has been through significant technological advancements in recent decades, leading to its widespread utilization in the treatment and diagnosis of urinary tract pathologies. Among them is its wide application in Retrograde IntraRenal Surgery. Nonetheless, laser fiber degradation and ureterorenoscope damage remain a significant concern. Mues et al.¹ expressed the degradation of the fiber tip as “burn back” that inevitably occurs during a stone surgery and has been reported as one of the leading causes of reduced ureterorenoscope durability. On the other hand, Talso et al.² showed that the bubble generated by the laser did not rebound on the ureterorenoscope camera when the laser fiber reached a quarter-point of the endoscopic view from the lateral side of the monitor. This phenomenon was described as a 'distance concept' which can prevent endoscope damage. So far, there have been several attempts to develop ureterorenoscope damage solutions. For instance, in a previous investigation, the authors demonstrated how to reduce scope damage by evaluating the relationship between laser fiber core degradation and fiber jacket burn.³

In previous study, we reported laser fiber degradation that occurred in multiple sites of the laser fiber tip; a phenomenon described as ‘double-firing,’ and it was pointed out as one of the leading causes of endoscopy failure as laser emission occurred inside the endoscope working channel.³ To the best of our knowledge, before this investigation, there was no published article about laser emission and damage on multiple laser fiber sites or the pattern of the laser fiber damage. Therefore, in the present study, the presenting authors classified and analyzed the different patterns of laser fiber degradation according to the laser settings. Furthermore, we also examined the movement of the cavitation bubbles and how it may affect fiber damage. We believe it is essential to understand the mechanism of the various causes of laser fiber damage and an ideal method of reducing endoscope damage induced by laser emission in multiple sites. Some surgical principles will be summarized accordingly.

METHODS

The authors initially obtained images from 118 samples of the laser fibers and analyzed the degradation patterns under several energy settings using 100W Ho:YAG laser (Versapulse suite, Lumenis, Yokneam, Israel). Pulse widths were about 750 μ sec, according to the information provided by the company. Laser fibers (Boston Flexiva, Boston Scientific, Marlborough, MA, USA) were cut every 3 cm from the tips and observed after stone fragmentation for one, three, and five minutes. Laser fibers with 200 μ m or 365 μ m were used in a hand-made benchtop model for the most widely used laser fibers in flexible endoscopes and related to breakdown of flexible endoscope. We used cubic-shaped 4 \times 4 \times 4 mm phantom stones with a powder-to-water mixing ratio of 15:3 with properties similar to calcium oxalate monohydrate stones in humans regarding the mean values, which were manufactured in the previously described method.^{3,4} Four phantom stones were used at once, and during the production of this phantom, the stones were all the same size. The weight of the phantom was measured to make the total amount the same as possible. The stones were fragmented with a hand-held maneuver to maintain the exact distance between the laser fiber tips and the phantom stones, mimicking the actual situation of endoscopic stone fragmentation. The benchtop model used in the experiment has a fixture that fixes the laser fiber, so the distance was maintained. When the fiber tip was worn and the distance from the stone increased, the laser fiber was pushed little by little as much as it was worn out.

Benchtop model

To reproduce a similar situation to the pop-dusting stone fragmentation in a human calyx of the kidneys, a 3D printed benchtop model was manufactured and used in the laboratory; the benchtop had a slope of approximately 25 degrees to mimic the upper pole calyx of the kidneys when the patient lies in the Trendelenburg position.³ The fiber tip and phantom stones were maintained in 0.9% normal saline with continuous flow irrigation (Supplementary Fig. 1).

Laser fiber collection and the laser setting

Before performing lithotripsy, every 3cm from the fiber tip was marked. Fiber diameters of 200 μm and 365 μm were used, and 1-, 3-, and 5-min laser emissions were performed in the groups of 1minGr, 3minGr, and 5minGr, respectively. Laser emission was done under four different energy settings (1 J-10 Hz, 1 J-20 Hz, 1 J-30 Hz, and 2 J-10 Hz) in the group 3minGr. The setting of 1 J-10 Hz in the group 1minGr was added and tested as the negative control to tell the differences from the groups 3minGr and 5minGr. The 2 J-10 Hz is not a routine setting during the stone surgery with the 200- and 365- μm fibers, and it can be used for selected cases during a pop-dusting technique. Therefore, 1 J-10 Hz, 1 J-20 Hz, 1 J-30 Hz settings were tested in the group of 5minGr as the positive control. The laser fibers were cut with CS-124 ceramic scissors (Kyocera, Kyoto, Japan) with the span of the previously marked 3 cm.

Inspection of the shortened laser fiber and the cavitation bubbles

The authors captured the remnant laser fibers photos after magnifying 230 times using a digital microscope (AD7031MZT, Dino-lite, Taipei, Taiwan). The degraded length was measured by making marks at intervals of 3 cm and subtracting the remaining length from 3 cm after stone fragmentation. Then, the fiber jackets were stripped off using a fiber stripper, and photos of the damaged areas were obtained. A high-speed camera (V642; Vision Research Inc., Wayne, NJ, USA) and a lens (105 mm; Nikon, Tokyo, Japan) at a rate of 7,500 images per second in full format and 200,000 images at a resolution of 128 \times 128 pixels (128 \times 64 pixels at 360,000 images) to analyze how the damage occurred and visualize the cavitation bubbles. In addition, we took photos of the movement of the cavitation bubbles. At the same time, we apply the polyacrylamide polymer gel with a distance of 1 to 5 mm in front of the laser fiber tip.

Statistical analysis

According to each laser setting and the fiber caliber, the statistical analysis was performed on the pattern damage; ANOVA for non-continuous variables and independent *t*-test for continuous variables were used with the post-hoc analysis. IBM-SPSS statistics 25.0 (IBM, Armonk, NY, USA) was used for statistical analysis.

RESULTS

After inappropriate fiber segments were excluded from the analysis, we examined a total of 100 laser fibers. The types and the characteristics of damage were examined by two independent reviewers (Lee SM, So SW), and similar damage patterns were grouped at first. If there was a difference of opinion, reviewers discussed the pattern of damage, and as a final agreed conclusion, 7 types of damage were derived. Seven types of degradation patterns were observed from the laser fiber samples and classified based on prominent degradation features: 1) 'Charring' indicated the laser fiber with black burned areas at the laser fiber tips; 2) 'Limited peeled-off' indicated a situation when the laser fiber is peeled, and the longest

length of the peeled portion is shorter than the diameter of the fiber; 3) Conversely, was when the longest length of the peeled portion was longer than the diameter of the fiber, the authors called it 'Extensive peeled-off'; 4) 'Bumpy' indicated uneven degradation of the laser fiber tip like apple bites; 5) An opaque surface in the fiber glasses referred to 'whitish plaque'; 6) 'Crack' indicated the linear fracture of the laser fiber with partial continuity of the fiber; 7) 'Break-off' indicated a situation when the laser fiber was divided into two or more pieces (Fig. 1). Eighty-seven charrings, 66 limited peeled-offs, 79 cases of extensive peeled-offs, 35 bumpies, 45 cracks, 8 break-offs, and 43 whitish plaques were observed (Table 1). There were no differences between the laser fibers of 200 μm and 365 μm regarding the shortened lengths and the seven types of the laser fiber degradation patterns (Table 2).

There were no significant statistical differences between the mean laser lengths of 28.82 ± 0.73 mm and 28.65 ± 0.92 mm in the groups 1minGr and 3minGr, respectively ($P = 0.835$). The mean laser length of the group 5minGr was 26.11 ± 1.91 mm, and it was significantly shorter than the other groups ($P < 0.001$). The shortened fiber lengths according to the laser setting or the diameter of the fibers were not different across the groups.

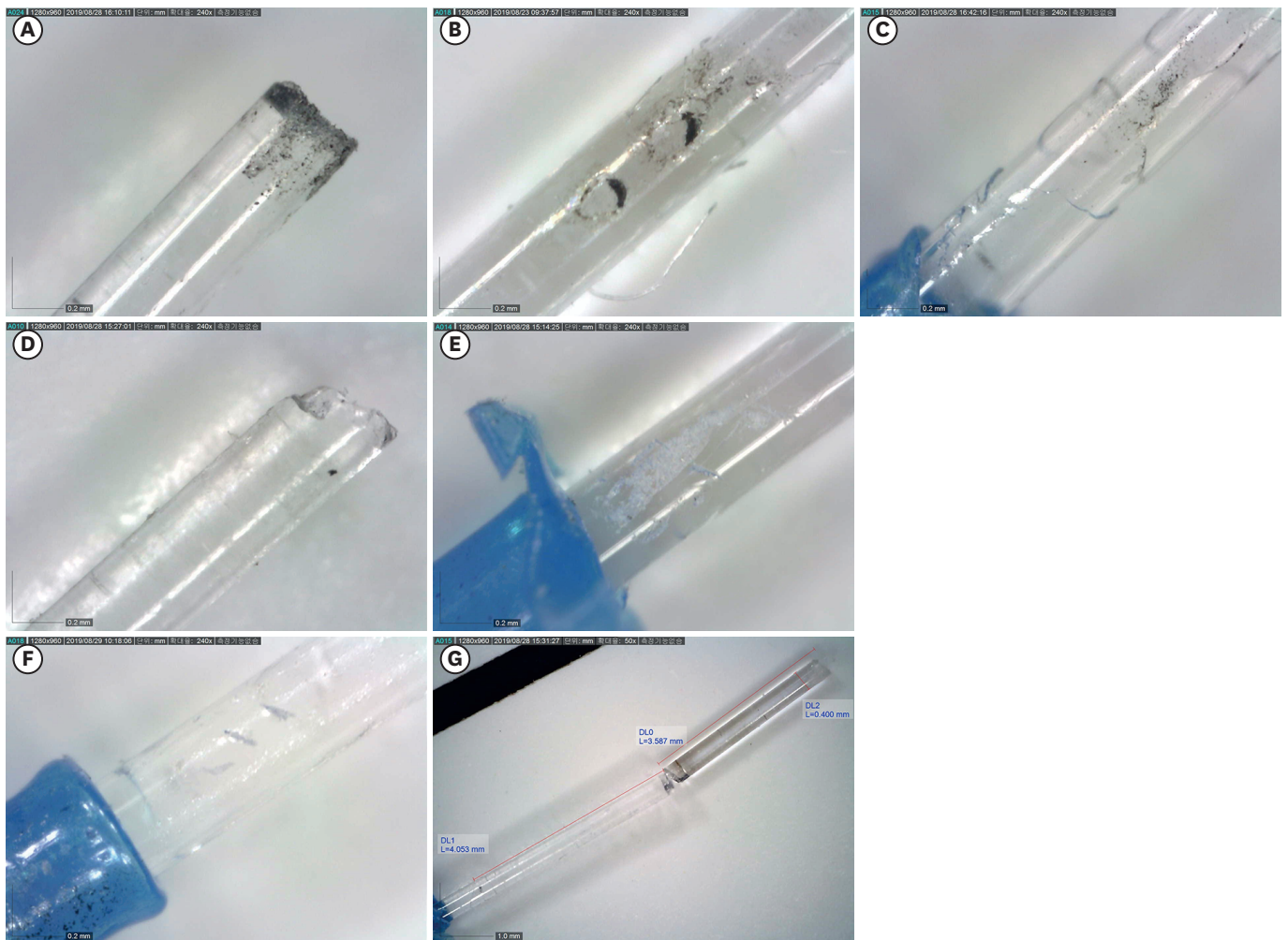


Fig. 1. Patterns of laser fiber degradation. Types of laser fiber damages. (A) Charring, (B) Limited peeled off, (C) Extensive peeled off, (D) Bumpy, (E) Bumpy, (F) Crack, (G) Break off.

Table 1. Damage pattern distribution according to the time of the laser emission and the laser setting

Time	Laser setting	Charring	Limited Peeled off	Extensive Peeled off	Bumpy	Whitish plaque	Crack	Break off	Fiber length (mm)
1 min	1 J, 10 Hz (n = 20)	9 (45%)	6 (30%)	19 (95%)	9 (45%)	11 (55%)	2 (10%)	0 (0%)	28.82 ± 0.73
3 min	1 J, 10 Hz (n = 20)	15 (75%)	15 (75%)	15 (75%)	7 (35%)	7 (35%)	8 (40%)	1 (5%)	28.95 ± 0.98
	1 J, 20 Hz (n = 20)	19 (95%)	12 (60%)	14 (70%)	7 (35%)	11 (55%)	10 (50%)	1 (5%)	28.58 ± 0.51
	1 J, 30 Hz (n = 19)	19 (100%)	17 (89%)	14 (74%)	5 (26%)	8 (42%)	9 (47%)	0 (0%)	28.83 ± 1.07
	2 J, 10 Hz (n = 19)	17 (89%)	13 (68%)	16 (84%)	6 (32%)	9 (47%)	7 (37%)	2 (10%)	28.22 ± 0.93
	Sum (n = 78)	70 (90%)	57 (73%)	59 (76%)	25 (32%)	35 (45%)	34 (44%)	4 (5%)	28.65 ± 0.92
5 min	1 J, 10 Hz (n = 10)	9 (90%)	5 (50%)	10 (100%)	6 (60%)	7 (70%)	4 (40%)	0 (0%)	27.75 ± 1.05
	1 J, 20 Hz (n = 5)	4 (80%)	3 (60%)	5 (100%)	4 (80%)	4 (80%)	1 (20%)	1 (20%)	24.90 ± 0.50
	1J, 30Hz (n = 5)	4 (80%)	2 (40%)	5 (100%)	2 (40%)	4 (80%)	1 (100%)	0 (0%)	24.04 ± 0.86
	Sum (n = 20)	17 (85%)	10 (50%)	20 (100%)	12 (60%)	15 (75%)	6 (30%)	1 (5%)	26.11 ± 1.91

Table 2. Damage pattern distribution according to the caliber

Diameters of laser fibers	Charring	Limited Peeled off	Extensive Peeled off	Bumpy	Whitish plaque	Crack	Break off	P value
200 um (n = 38)	34 (89%)	33 (87%)	25 (66%)	16 (42%)	21 (55%)	18 (47%)	3 (8%)	0.227
365 um (n = 40)	36 (90%)	24 (60%)	34 (85%)	9 (23%)	14 (35%)	16 (40%)	1 (3%)	

The occurrence rates of 7 types of fiber degradation

The occurrence rates (Table 3) of charring were 45.0%, 89.7%, and 85.0% in groups 1minGr, 3minGr, and 5minGr, respectively ($P < 0.001$). The occurrence rates of limited peeled-off and the extensive peeled-off was 30.0%, 73.1%, and 50.0% ($P = 0.001$), and 95.0%, 75.6%, and 100.0% ($P = 0.010$) in groups 1minGr, 3minGr, and 5minGr, respectively. Subgroup analysis showed that limited peeled-off occurrence rates were significantly higher in groups 3minGr and 5minGr than in group 1minGr. The extensive peeled-off occurrence rates were significantly lower in group 3minGr than in the other groups. The occurrence rates of the bumpy was 45.0%, 32.1% and 60.0% ($P = 0.061$) and that of the whitish plaque was 55.0%, 44.9% and 75.0% ($P = 0.053$) in the groups 1minGr, 3minGr, and 5minGr, respectively. Comparing groups 3minGr and 5minGr, the occurrence rates of the bumpy ($P = 0.037$, hazard ratio = 3.2) and the whitish plaque ($P = 0.023$, hazard ratio = 3.7) were significantly higher in the 5minGr than in the 3minGr group. The occurrence rates of the crack were 10.0%, 43.6%, and 30.0% in groups 1minGr, 3minGr, and 5minGr, respectively ($P = 0.057$); its occurrence rate was significantly higher in the 3minGr and 5minGr groups than in the 1minGr group ($P = 0.017$). The occurrence rates of the break-off were 0%, 5.1%, and 5.0% in the groups 1minGr, 3minGr, and 5minGr, respectively ($P = 0.587$).

Table 3. The occurrence rates of 7 types of fiber degradation

Laser fiber damage according to the firing time	1 min	3 min	5 min	P value
All settings				
Charring	45.0%	89.7%	85.0%	0.000
LPO	30.0%	73.1%	50.0%	0.001
EPO	95.0%	75.6%	100.0%	0.010
Bumpy	45.0%	32.1%	60.0%	0.061
Crack	10.0%	43.6%	30.0%	0.057
Break off	0%	5.1%	5.0%	0.587
Whitish plaque	55.0%	44.9%	75.0%	0.053
10 Hz group				
Charring	45.0%	87.2%	90.0%	0.001
LPO	25.0%	82.1%	50.0%	0.000
EPO	95.0%	74.4%	100.0%	0.040
Bumpy	45.0%	30.8%	60.0%	0.196
Crack	10.0%	43.6%	40.0%	0.031
Break off	0%	2.6%	0%	0.677
Whitish plaque	55.0%	38.5%	70.0%	0.153

LPO = limited peeled off, EPO = extended peeled off.

The occurrence rates of all the fiber degradation types were not significantly different across the laser settings in groups 3minGr and 5minGr.

The damaged lengths and the cavitation

The damaged lengths of the remnant laser fibers in group 3minGr were 5.10 ± 1.25 mm in total. The damaged lengths were 5.71 ± 1.59 mm, 5.36 ± 1.27 mm, 4.48 ± 0.82 mm, and 4.78 ± 0.78 mm under energy settings of 1 J-10 Hz, 1 J-20 Hz, 1 J-30 Hz, and 2 J-10 Hz respectively in the group 3minGr ($P = 0.006$). Subgroup analysis showed that the damaged lengths under energy settings of 1 J-10 Hz were significantly longer than those in the other groups ($P = 0.038$). However, the shortened length of 2 J-10 Hz was not significantly longer than others at 3 minGr ($P = 0.090$). The cavitation size of 1 J and 2 J were 4–5 mm and 6–7 mm, respectively (Fig. 2). When there is a tissue-mimicking gel in front of the laser fiber tip, the backward movement of the cavitation bubbles was found when the distance is 1 mm, not 2 mm to 5 mm (Fig. 3). Cavitation with heated bubbles occurred around the tip of the laser fiber, and the damaged lengths were deeper than the diameters of the cavitation bubbles because of its movement to the proximal part of the laser fiber.

DISCUSSION

Since lithotripsy with the pulsed-dye holmium-YAG laser has been used for urinary stone fragmentation, there have been numerous studies to understand fiber degradation.⁵ To the best of our knowledge, 100 samples were analyzed for typical characteristics of laser fiber degradation, and the different types of degradation were classified using acceptable criteria for the first time in the world. In addition, the authors considered the visible, distinct pattern of the laser fiber degradation and the clinical importance of the relationship between the patterns of laser fiber damage and the possible risk of endoscopic damage.^{6,7} We believe that it would be helpful to understand why laser fiber degradation occurs at the fiber tip, how the laser emission occurs in multiple sites, what laser setting would provide optimal conditions for reducing scope damage, the best time to cut the fiber tip, how much the fiber should be cut, and how much the laser fiber should be advanced from the tip of the ureterorenoscope according to the location of the stones in the kidney.

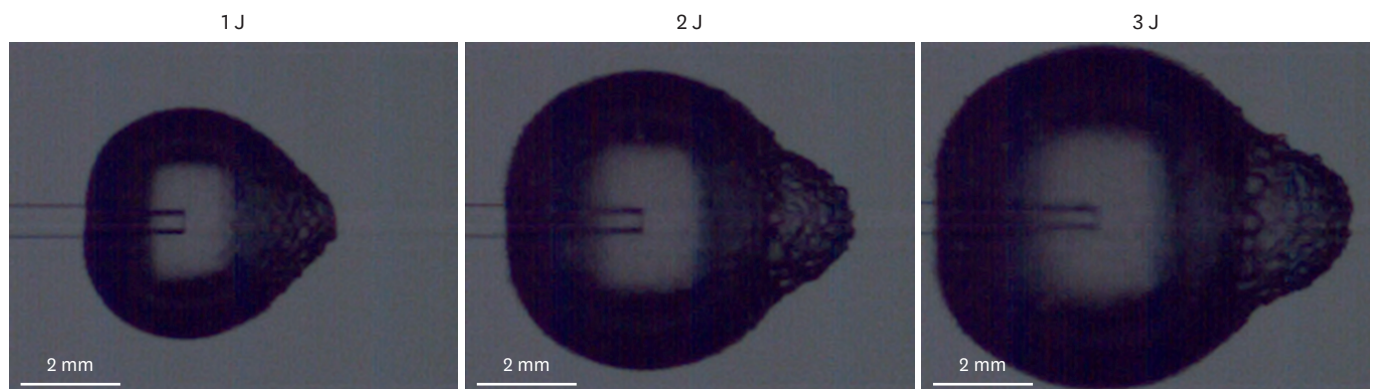


Fig. 2. Cavitation around the tip of the laser fiber. Single shot of laser emission with the energy of 1 J, 40,000 frames per second, and 1 microsec minimum exposure time.

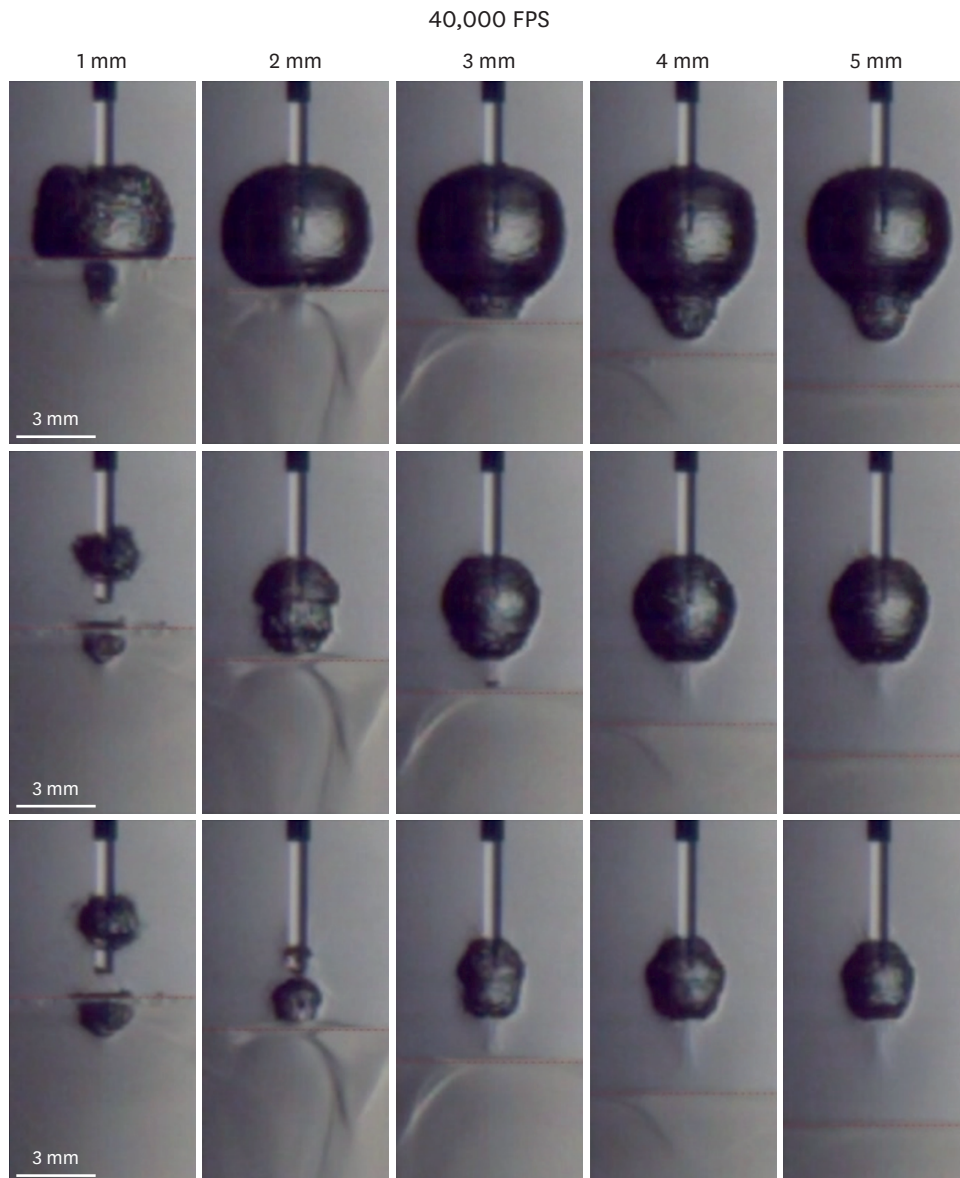


Fig. 3. Size differences of cavitation bubbles according to the laser power (J). Migration of the bubbles at the distance of 1 mm.

Heat damage of the cavitation bubbles and backward movement at a 1 mm distance from the stone

All types of laser fiber degradation seem to correlate with energy transmission in the laser fiber. Laser-induced cavitation typically generates volumetric heat deposition in water of 6,000 to 15,000°C and thermal expansion of heated bubbles in front of the laser fibers tip as shown in Fig. 2.^{8,9} The heat can cause carbonization of the fiber tips (charring) and fiberglass degradation (bumpy). The heated bubbles may expand and then collapse while causing impingement of water jets penetrating inside the bubbles to the surface of the laser fibers. This water jet can randomly cause fiber degradation such as limited peeled-off, extensive peeled-off, whitish plaque, crack, and break-off. A previous study⁸ showed the plasma bubble formation induced by Ho:YAG laser in an intro study. However, the Fig. 2 of this study described the bubble formation in front of the tip of the laser fiber and not “on” the laser

fiber. They focused on the high temperature only. Therefore, it could not explain why the bubble could damage the surface and the body of the laser fibers.

More importantly, we must concentrate on the discrepancy between the lengths of the fiber damage and the bubble size. The diameter of the cavitation bubble of 1 Hz in Fig. 2 was 5 mm to 6 mm, and the area covered by the bubble was 3–4 mm. This length is almost the same as the damaged lengths of the laser fibers, especially when we consider the backward migration of the bubbles with the distance of 1 mm from the target. The cavitation bubble seems to move to the distal tip of the fiber when it is bumped against the stones or the mucosa wall. And the renal stones in the patients may not lie horizontally and the backward and upward movement of the cavitation bubbles can be enhanced if the laser fiber goes downward to the stones in the upper pole calyces. Now, the present study could find why the proximal part of the laser fiber can be damaged and why the damaged segment can be longer than the maximal diameter of the bubbles for the first time in the stone surgery using the flexible ureterorenoscope. It was because of the backward migration of the bubbles. **Supplementary Video 1** helps understanding the formation of cavitation bubble and damage to laser fiber.

Coincidence of multiple damages at the fiber surface

Multiple damage occurred according to time sequence, and interestingly, the authors observed that the fiber damages did not occur in a specific order. Multiple damages coincide at the fiber surface. These multiple damages were presented numerically in the **Table 1**, and additional analysis at **Table 3** was performed to determine which damage patterns became more pronounced according to the time of 1, 3, and 5 minutes. As a result, it was possible to presume what kind of damage more would occur over time. The fibers were rapidly shortened after 3-min of laser emission, and the laser fibers at 5-min emission were significantly shorter than those at 1- and 3-min emission. The peeled-off was frequently found at 3- and 5-min laser emission in many sites, and no differences were found between 3- and 5-min laser emission. This could imply that the peeled-off is not a sequential damage process. The whitish plaque was found more frequently at 5-min emission than 3-min emission, and it may be a cause of the rapid shortening of the laser fiber after 3-min laser emission.

The crack and the break-off correlate with laser fiber continuity, and the ‘double-firing phenomenon’ in the previous investigation may have been derived from the crack of the fiber.³ It could be a dangerous signal for break-off of the laser fiber especially when it occurs inside the working channel of the endoscopy. The crack frequently occurred at 3- and 5-min laser emission, and it is similar to the actual clinical setting in the operation room. Maximal deflection to the lower pole of the kidneys can cause additional damage to the laser fiber.¹⁰ However, it does not seem to be related to the occurrence of the ‘double-firing phenomenon’ because it usually appears after several minutes during stone fragmentation.

The fiber length was independent of the damage type. The present authors could recognize that peel-off damage occurred on the fiber’s surface, and the fibers’ shortening could occur differently apart from peel-off damage. The bumpy effect could break the fiber tip, but it was not the ‘complete shortening’ of the fiber. Instead, the bumpy showed partial destruction of the fiber tip, and the authors inevitably measured the length from the intact part of the laser fiber tip. This finding may mean that the shortening and destruction of the fiber tip occur with the energy transmission, and the laser fiber tip may shatter into splinters and tiny particles in the water.

Lessons from the analysis of laser fiber damage

Based on the findings of the present study, the authors would recommend some suggestions to reduce damage of the laser fibers and the endoscopes. The recommendations might help the surgeons to improve the durability of the endoscope and increase the efficiency of stone surgery (Fig. 4).

- 1) Minimum distance of 5 mm: The ideal mean distance from the laser fiber tip to the endoscopy should be at least 5 mm considering the damaged lengths of the remnant laser fibers in group 3minGr (Fig. 4A). It seems to be related to the area of the heated bubbles in Fig. 2.
- 2) Advancement of the laser fiber first, later cutting: If the 'double-firing phenomenon' is identified, the laser fiber must have cracked with a risk of a break-off. Therefore, the laser fiber should be moved forward longer than 5 mm inside the calyx, or the tip of the laser fiber should be cut. However, cutting the laser fiber is a time-consuming task for surgeons. Therefore, the authors think that forward movement of the laser fiber is more recommendable than the fiber-cutting procedure.
- 3) Frequent cutting in specific conditions: The laser fiber cannot be advanced longer than 3mm from the tip of the flexible ureteroscope to reach the stone when the laser fiber almost escapes from the stone because of the acute deflection angle. The problems may occur in a lower pole stone with a narrow infundibulopelvic angle (Fig. 4A), stones in a diverticular space (Fig. 4B), or stones in the duplicated kidneys. At this time, surgeons have to cut the laser fiber frequently to prevent the damage of the laser fiber. The laser fiber should be cut at around 3-min continuous laser emission for stone fragmentation, and the length to cut should be 5 mm regardless of the laser setting. In the previous study, the authors recommended 1 or 2 mm proximal level from the black burned part of the blue colored-laser fiber jacket.³
- 4) > 5 mm distance with damaged fibers: Another essential thing is that we have to advance the laser fiber into the target until we can see the intact proximal part of the laser fiber even the length is already > 5 mm (Fig. 4C-F).
- 5) Laser setting: No statistically significant differences were identified across the laser setting of 1 J-20 Hz, 1 J-30 Hz, and 2 J-10 Hz at three min of laser emission ($P = 0.090$). However, 1 J-20 Hz (Fig. 4C and D) showed longer remnant laser fibers than 1J-30Hz or 2J-10Hz at the laser emission of 5minGr (Fig. 4E and F).
- 6) Safety distance > 1 mm from the stone: Contact mode or < 1 mm distance of the laser fiber from the stone can induce backward movement of the cavitation bubbles, and the risk of damage may increase. It would be helpful for surgeons to keep in mind that the safety distance is > 1 mm from the stone during the pop-dusting technique. The finding in a previous study² was partially correct because the bubbles generated by the laser could rebound on the ureterorenoscope camera even when the laser fiber reached a quarter-point of the endoscopic view from the lateral side of the monitor if the fiber is located at the 1 mm distance from the stone. However, it should be noted that at a distance of > 1 mm, the light transmittance starts to drop significantly to 30%, which eventually prolongs the procedure time, which may reduce the stone removal efficiency.
- 7) The blue-colored fiber jacket should not be stripped off before the stone surgery, although the protective effect of the fiber jacket from peeled-off, whitish plaque, crack, and the break-off has not yet been tested. The presenting authors found that almost all cases of break-off in this study maintained the alignment of the laser fiber inside the blue jacket, and the 'double-firing' signal or black-colored burned part can be important warning signs in preventing the endoscopic damage resulting from the break-off (Fig. 4D, E, and F).

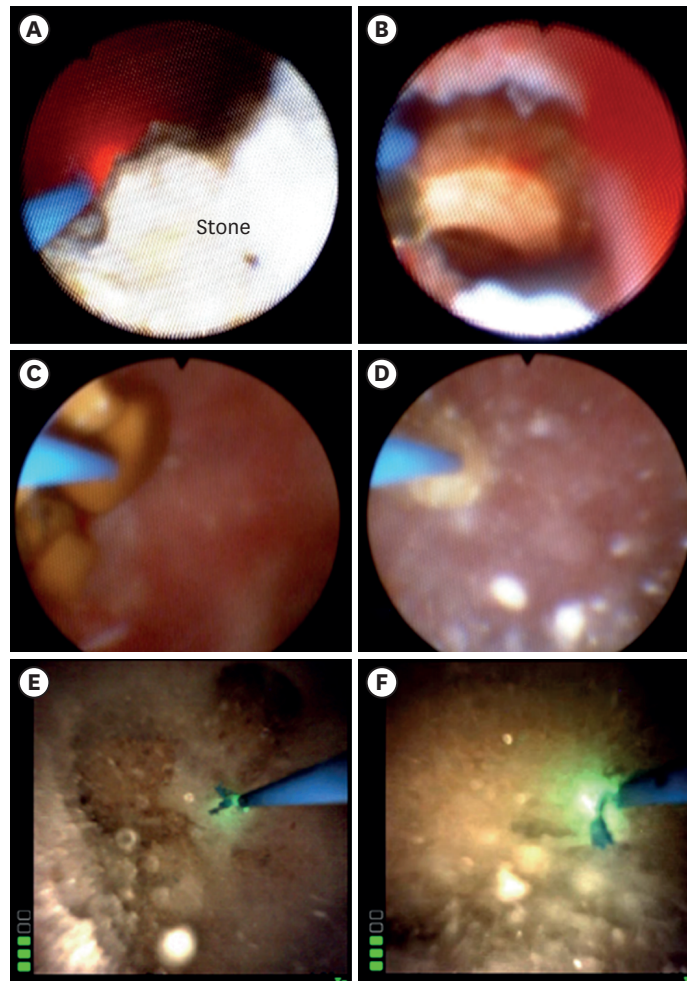


Fig. 4. Laser tip during flexible ureteroscopic surgery. The laser fiber cannot be advanced > 3 mm from the tip of the flexible ureteroscope to reach the stone when the laser fiber almost escapes from the stones because of the acute deflection angle in a lower pole (A) or in a diverticular space (B). Change in the lengths of the intact part of the laser fibers are shown before and after pop-dusting techniques for 5 minutes. The laser setting of 1 J-20 Hz (C, D) showed longer remnant laser fibers than 1 J-30 Hz (E, F).

- 8) The energy from the light cable can deliver additional heat to the water before the endoscopy. Therefore, cool water irrigation with high velocity might be helpful to cool down the water and forward movement of the cavitation bubbles. Warm irrigation fluid should not be used.

Limitation

This study has some limitations. First, the sample size is small. However, it was a reproducible experiment, with 1- and 5- min data negative and positive controls respectively to tell the differences of the results compared to those of 3-min laser emission. The occurrence of cavitation bubbles was also examined, and there are important lessons from the experiment on improving the durability of endoscopy. Second, the presenting authors could not find the sequential fiber degradation process because of the technical limitation of the recording method that was used to evaluate all the fiber surface degradation processes. Third, the experiment was performed in vitro with phantom stones. The real-world data could be different with confounding factors such as anatomical variation, usage of irrigation

fluid, mishandling of the laser fiber outside the endoscopy, and laser settings among others. The presenting authors tried to set the experiment conditions as close as possible to the situation in the operating room. Fourth, Mues et al.¹ described laser fiber degradation and energy transmission vary across manufacturers and laser fiber types. Although Boston Scientific's laser fiber was used in this study, it would be meaningful to analyze and compare the laser fiber degradation pattern with laser fibers from different manufacturers and fiber materials. Lastly, the authors could not find any danger signal except for the double-firing phenomenon helpful in detecting the broken laser fiber.

Conclusion

After the authors reviewed all the damage patterns of the laser fiber tips, we could classify them into seven types. The heat damage around the surface of the laser fiber can be increased according to the high-energy or high-frequency laser setting, a short distance to the stone, a short distance from the tips of flexible ureteroscopes, no cutting laser fiber procedures, and the inappropriate use of irrigation fluid or laser fiber jacket.

SUPPLEMENTARY MATERIALS

Supplementary Fig. 1

Experimental device for stone fragmentation. (Left) Hand-held stone fragmentation, (Right) Fixed-laser stone fragmentation.

[Click here to view](#)

Supplementary Video 1

Laser-induced cavitation formation.

[Click here to view](#)

REFERENCES

1. Mues AC, Teichman JM, Knudsen BE. Quantification of holmium:yttrium aluminum garnet optical tip degradation. *J Endourol* 2009;23(9):1425-8.
[PUBMED](#) | [CROSSREF](#)
2. Talso M, Emiliani E, Haddad M, Berthe L, Baghdadi M, Montanari E, et al. Laser fiber and flexible ureterorenoscopy: the safety distance concept. *J Endourol* 2016;30(12):1269-74.
[PUBMED](#) | [CROSSREF](#)
3. Ryang SH, Ly TH, Yoon HS, Park DH, Cho SY. How to reduce 'double-firing'-induced scope damage by investigating the relationship between laser fiber core degradation and fiber jacket burn? *PLoS One* 2020;15(5):e0233135.
[PUBMED](#) | [CROSSREF](#)
4. Lee JW, Park MG, Cho SY. How to perform the dusting technique for calcium oxalate stone phantoms during Ho:YAG laser lithotripsy. *BMC Urol* 2018;18(1):103.
[PUBMED](#) | [CROSSREF](#)
5. Denstedt JD, Razvi HA, Sales JL, Eberwein PM. Preliminary experience with holmium: YAG laser lithotripsy. *J Endourol* 1995;9(3):255-8.
[PUBMED](#) | [CROSSREF](#)
6. Sooriakumaran P, Kaba R, Andrews HO, Buchholz NP. Evaluation of the mechanisms of damage to flexible ureteroscopes and suggestions for ureteroscope preservation. *Asian J Androl* 2005;7(4):433-8.
[PUBMED](#) | [CROSSREF](#)

7. Landman J, Lee DI, Lee C, Monga M. Evaluation of overall costs of currently available small flexible ureteroscopes. *Urology* 2003;62(2):218-22.
[PUBMED](#) | [CROSSREF](#)
8. Cecchetti W, Zattoni F, Nigro F, Tasca A. Plasma bubble formation induced by holmium laser: an in vitro study. *Urology* 2004;63(3):586-90.
[PUBMED](#) | [CROSSREF](#)
9. Sinibaldi G, Occhicone A, Pereira FA, Caprini D, Marino L, Michelotti F, et al. Laser induced cavitation: plasma generation and breakdown shockwave. *Phys Fluids* 2019;31(10):103302.
[CROSSREF](#)
10. Forbes CM, Rebullar KA, Teichman JM. Comparison of flexible ureteroscopy damage rates for lower pole renal stones by laser fiber type. *Lasers Surg Med* 2018;50(8):798-801.
[PUBMED](#) | [CROSSREF](#)